

**Reaction-subdiffusion model of morphogen gradient formation**S. B. Yuste,<sup>1</sup> E. Abad,<sup>1</sup> and Katja Lindenberg<sup>2</sup><sup>1</sup>*Departamento de Física, Universidad de Extremadura, E-06071 Badajoz, Spain*<sup>2</sup>*Department of Chemistry and Biochemistry and BioCircuits Institute, University of California–San Diego, 9500 Gilman Drive, La Jolla, California 92093-0340, USA*

(Received 1 August 2010; revised manuscript received 18 November 2010; published 14 December 2010)

We study gradient formation of subdiffusive morphogens. The morphogens are produced at a source point at a constant rate. From there they move subdiffusively and are also subject to degradation at a rate that may depend on location and on time. Our analysis is based on a reaction-subdiffusion equation obtained from a continuous time random-walk model with a long-tailed waiting time distribution that also incorporates an evanescence process. Spatially uniform degradation at a constant rate leads to an exponentially decreasing stationary concentration profile hardly distinguishable from that obtained with normal diffusion. On the other hand, with location-dependent degradation we find a rich gamut of profiles, some qualitatively quite different from those occurring with normal diffusion. We conclude that long-time morphogen concentration profiles are very sensitive to the spatial dependence of the reactivity and may also serve as a sensitive measure of the occurrence of anomalous diffusion.

DOI: [10.1103/PhysRevE.82.061123](https://doi.org/10.1103/PhysRevE.82.061123)

PACS number(s): 05.40.–a, 82.39.–k, 82.40.Ck, 87.17.Pq

**I. INTRODUCTION**

The spatial distribution, differentiation, and further development of many embryonic cells is governed by the spatial distribution of special signaling molecules called morphogens. A role of morphogen gradients in developmental biology has been accepted for decades, including the classic paper of Crick [1]. However, only in the past decade have experiments made possible the understanding of ways in which cells can sense and respond to extremely small changes in even very low concentrations of extracellular signaling factors [2].

Standard models of morphogen gradient formation assume that a specific part of the embryo secretes morphogens at a constant rate. The secreted morphogens then undergo degradation as they disseminate through the tissue, resulting in a concentration gradient. Different target genes in the embryonic cells are activated when the morphogen concentration exceeds a specific threshold for that gene, thus leading to a cell response to the local environment that depends on the local concentration. Because of this differential response, cells are able to interpret the morphogen gradient and translate it into specific “code” for their subsequent development via the expression of relevant genes.

Traditional models of morphogen gradient formation are based on diffusion equations with an added linear degradation term and a localized source of morphogen molecules [3]. Such ordinary diffusion equations arise from continuous time random walks (CTRWs) with exponentially decaying or other short-tailed waiting time distributions. However, there are at least two oversimplifications in this formulation. On the one hand, the morphogen gradient produced by a degradation process that is independent of location is not well buffered against inevitably occurring genetic and environmental fluctuations [4]. Such buffering is of course a requirement for the stability of any mechanism of cell differentiation and genetic development. One way to achieve buffering is for the morphogens to decay rapidly close to their source

but more slowly farther away [4]. It is thus important to explore a variety of degradation mechanisms. Furthermore, the consequences of different degradation mechanisms depend on the details of the morphogen transport mechanism [5]. One of the factors affecting morphogen transport is the nature of the environment. The complexity of biological environments may result in morphogenic species encountering a large number of obstacles, barriers, traps, and other impediments in the course of their trajectories, leading to anomalous transport [6], more specifically, to subdiffusion. For example, it has recently been argued that for morphogens such as decapentaplegic (Dpp), wingless (Wg), and hedgehog (Hh) the proteins of the heparan sulphate proteoglycan (HSPG) family act as active obstacles where the morphogens are stalled with long-tailed waiting time distributions [7]. CTRWs with such long-tailed distributions are subdiffusive (see below).

In this paper we study morphogen gradient formation in subdiffusive media in which morphogen degradation may depend on position (and, in principle, also on time). Our goal is to show that the profile of the gradient may be sensitively dependent on the nature of the motion of the morphogens in the medium as well as on the degradation mechanism. We will show that in some cases where a stationary gradient exists in a diffusive medium, there is no stationary gradient in the subdiffusive counterpart. Morphogen gradients may therefore provide a sensitive indicator of the nature of the medium and of the degradation process. Our analysis starts with a well-known description of anomalous diffusion, namely, a CTRW, where the morphogen particles are characterized as random walkers. We base our analysis on an extension of the CTRW model to include degradation, followed by a coarse graining of the problem to arrive at a fractional reaction-subdiffusion equation. Our contribution is the derivation and solution of this equation for a number of different degradation mechanisms, and a detailed analysis of the resulting morphogen profiles. We restrict much of our discussion to one dimension not only for mathematical convenience but because in fact most experimental geometries for

this problem are effectively one-dimensional. In two-dimensional experiments the morphogen source is usually a line and in three-dimensional ones it is usually a surface, rendering an effectively one-dimensional geometry (see, e.g., the discussions in [7,8] and references therein).

While our discussion here revolves around morphogen gradient formation, we stress that our results are more generally applicable to any problem involving a source of particles that then move subdiffusively (as described by a long-tailed CTRW model) and are subject to a degradation process [9]. For example, our discussion could be relevant to the problem of controlled-release and microfluidic drug delivery technologies in tissue engineering [10]. It could also be relevant to point-source pollutants in groundwater when these pollutants can recombine or otherwise disappear. Similar additional examples can be found in [11] and references therein.

In Sec. II we present the model highlighting the principal steps used in deriving a fractional reaction-subdiffusion equation starting from a CTRW description that includes degradation. In Sec. III we detail the solution of this equation for various degradation profiles and compare and contrast the resulting morphogen gradients with those that would occur under the same degradation mechanisms if the motion of the morphogens were simply diffusive. The issue of robustness is considered in Sec. IV. We end with a summary and some remarks about future outlook in Sec. V.

## II. MODEL

To construct our model, we specify how the morphogens move in the medium, how they degrade, and how to combine these two dynamical contributions in a single evolution equation for the morphogen concentration as a function of location and time. There is an extensive recent literature on reactions in subdiffusive media, a great deal of it based on CTRW models and the associated integrodifferential equations. We particularly point to early work showing that subdiffusion stabilizes Turing patterns [12,13]. Other examples of derivations of reaction-subdiffusion equations based on CTRW models can be found in [14] for walks with internal dynamics and in [15] in the context of front propagation. Additional examples include [12,16–20].

Models of subdiffusion that are based on CTRWs start with particles described as random walkers whose jumps occur at times separated by idle time intervals drawn from a long-tailed waiting time distribution  $\psi(t)$ . In particular, for long times  $t$

$$\psi(t) \sim \gamma t_0^\gamma t^{-1-\gamma}, \quad (1)$$

where  $t_0$  is a constant that has dimension of time. The Laplace transform of  $\psi(t)$  is

$$\tilde{\psi}(u) \sim 1 - (\tau u)^\gamma \quad (2)$$

for small  $u$  with  $\tau^\gamma = \Gamma(1-\gamma)t_0^\gamma$ . The lengths of the jumps are characterized by a probability distribution function  $w(x)$  whose Fourier transform has the small- $q$  expansion

$$\hat{w}(q) \sim 1 - (\sigma q)^\mu. \quad (3)$$

For  $\mu < 2$ , the inverse Fourier transform of  $\hat{w}(q)$  for  $|x| \rightarrow \infty$  is

$$w(x) \propto \sigma^{-\mu} |x|^{-1-\mu}, \quad (4)$$

which has an infinite variance. The choice  $\mu=2$  (e.g., as in a Gaussian distribution of jump lengths or one with a constant jump length) corresponds to a finite jump length variance; specifically,  $\sigma^2$  is then half the variance of the jump length. When  $\gamma=1$  the mean time between jumps is finite, which is associated with normal diffusion. For our calculations in subsequent sections the jump length variance is finite and the mean time between jumps is infinite due to the presence of obstacles and traps, that is, we will take  $\mu=2$  and  $\gamma < 1$ .

The coefficients  $\sigma$  and  $\tau$  as well as the exponents  $\mu$  and  $\gamma$  are the microscopic parameters of the CTRW model. The mean-square displacement of these walkers with  $\mu=2$  grows sublinearly with time,

$$\langle x^2 \rangle \sim \frac{2K_\gamma}{\Gamma(1+\gamma)} t^\gamma. \quad (5)$$

Here  $K_\gamma$  is the subdiffusion coefficient related to the microscopic CTRW parameters by  $K_\gamma = \sigma^2 / \tau^\gamma$ . When  $\gamma=1$  (normal diffusion), an average over random-walk trajectories in the limit of long times and large displacements leads to the familiar classical diffusion equation. Instead, this limit for the power-law CTRW problem ( $\gamma < 1$ ) yields the fractional diffusion equation [9]

$$\frac{\partial c(x,t)}{\partial t} = K_\gamma {}_0D_t^{1-\gamma} \frac{\partial^2 c(x,t)}{\partial x^2}, \quad (6)$$

where  $c(x,t)$  stands for the morphogen concentration and  ${}_0D_t^{1-\gamma}$  is the Riemann-Liouville fractional derivative

$${}_0D_t^{1-\gamma} f(t) = \frac{1}{\Gamma(\gamma)} \frac{\partial}{\partial t} \int_0^t dt' \frac{f(t')}{(t-t')^{1-\gamma}}. \quad (7)$$

For normal diffusion this operator reduces to unity and one recovers the ordinary diffusion equation.

While this fractional subdiffusion equation can be taken as a starting point for the description of a number of biologically relevant problems [21], in the case of morphogens we must still incorporate the degradation process. This requires mathematical caution. For example, heuristic equations with separate added terms for the reaction and the transport processes lead to unphysical results such as negative particle concentrations (see, e.g., [22]). The correct derivation requires the reaction or degradation to be incorporated at a mesoscopic level of description. As we will see, a properly extended CTRW model leads to an equation which (in addition to a standard, purely reactive term) displays a mixed reaction-transport term containing both the reaction rate coefficient and a fractional derivative with respect to time [12,16–20].

To obtain a correct description of the evolution of the morphogen concentration, we follow an approach motivated by the derivation detailed in [16,23]. For this purpose it is

useful to first introduce some definitions and abbreviations. In particular, we define the operator  $\partial^\mu/\partial x^\mu$  via the relation

$$\mathcal{F}\left\{\frac{\partial^\mu g(x)}{\partial x^\mu}\right\} = -q^\mu \hat{g}(q), \quad (8)$$

where  $\mathcal{F}$  denotes the Fourier transform. When applied to a sufficiently well-behaved function  $g(x)$ ,  $\partial^\mu/\partial x^\mu$  is the Riesz fractional derivative [24]. Note that for  $\mu=2$  this is simply the Laplacian operator, which we will focus on later. We also note that the Laplace transform  $\mathcal{L}$  of the Grünwald-Letnikov fractional derivative is

$$\mathcal{L}\{{}_0D_t^{1-\gamma}f(t)\} = u^{1-\gamma}\tilde{f}(u), \quad (9)$$

which coincides with the Riemann-Liouville derivative [25] provided that  $f(t)$  is sufficiently regular at the origin [ $\lim_{t\rightarrow 0} \int_0^t d\tau(t-\tau)^{\gamma-1}f(\tau)=0$ ]. Our morphogen concentration function  $c(x,t)$  will be assumed to fulfill this condition.

We next need to describe the morphogen degradation mechanism. We assume the loss of particles at location  $x$  due *exclusively* to reactions to be given by

$$\left.\frac{\partial c}{\partial t}\right|_{\text{reaction}} = -k(x,t)c(x,t), \quad (10)$$

that is,  $k(x,t)$  is in general a location and time dependent decay rate coefficient. Note that this equation does not necessarily imply a first-order reaction since so far  $k(x,t)$  is not restricted and might itself depend on  $c(x,t)$  or on the concentration of some other species. For instance, there has been recent discussion of scaling of morphogen gradients relying on a feedback topology in which the range of the morphogen gradient increases with the abundance of some diffusible molecule whose production, in turn, is repressed by morphogen signaling [26]. The integrated form of Eq. (10),  $c(x,t')/c(x,t)=A(x,t,t')$ , with

$$A(x,t,t') = \exp\left[-\int_{t'}^t k(x,t'')dt''\right], \quad (11)$$

describes the time evolution of the ratio of the concentration of the particles at  $x$  at time  $t$  to the concentration at  $x$  at the initial time  $t'$  when the number of particles at  $x$  changes due exclusively to reactions, that is, when the changes in concentration at  $x$  caused by particle jumps into or out of  $x$  are not considered. Therefore  $A(x,t,t')$  can be thought of as the (survival) probability that a particle that is at  $x$  at time  $t'$  does not disappear from  $x$ , due exclusively to reaction, during the time interval  $t-t'$ .

Next we introduce  $j(x,t)$  and  $i(x,t)$ , respectively, the incoming and outgoing flux of particles at location  $x$  at time  $t$ . These two functions are related to one another,

$$j(x,t) = \int i(x-z,t)w(z)dz, \quad (12)$$

which simply states that the incoming flux at  $x$  at time  $t$  arises from the outgoing fluxes at all other locations  $x-z$  at that time. Since the morphogen concentration at  $x$  can only change due to the incoming and outgoing fluxes and due to

the degradation process at that location, we can write the balance equation

$$\frac{\partial}{\partial t}c(x,t) = j(x,t) - i(x,t) - k(x,t)c(x,t). \quad (13)$$

An additional relation connecting the fluxes and concentration is

$$i(x,t) = \psi(t)A(x,t,0)c(x,0) + \int_0^t \psi(t-\tau)A(x,t,\tau)j(x,\tau)d\tau. \quad (14)$$

This relation states that the outgoing flux from  $x$  at time  $t$  has two contributions. One arises from the particles that started out at  $x$  at time  $t=0$ , did not degrade or move anywhere up to time  $t$ , and then took a step away from  $x$  at time  $t$ . The second contribution arises from those morphogens that arrived at  $x$  at some earlier time  $\tau$ , waited there up to time  $t$  without degradation, at which point they stepped away.

Equations (12)–(14) provide all the necessary ingredients of the model. We now proceed to combine these contributions to arrive at a final reaction-subdiffusion equation. The balance Eq. (13) can be rewritten as

$$A(x,t,0)\frac{\partial}{\partial t}c^*(x,t) = j(x,t) - i(x,t), \quad (15)$$

where  $c^*(x,t) \equiv c(x,t)A(x,0,t)$ . Combining this with Eq. (12) leads readily to

$$A(x,t,0)\frac{\partial}{\partial t}c^*(x,t) = \mathcal{F}^{-1}\{[\hat{w}(q) - 1]\hat{i}(q,t)\},$$

$$\frac{\partial}{\partial t}c^*(x,t) = A(x,0,t)\sigma^\mu \frac{\partial^\mu}{\partial x^\mu}i(x,t), \quad (16)$$

where the second line follows from the first and the definition Eq. (8) of the Fourier transform. Upon Laplace transforming the second balance equation [Eq. (14)] with respect to time and then transforming back, the equation can be rewritten as

$$i(x,t) = A(x,t,0)\mathcal{L}^{-1}\left\{\frac{u\tilde{\psi}(u)}{1-\tilde{\psi}(u)}\tilde{c}^*(x,u)\right\}$$

$$= A(x,t,0)\tau^{-\gamma}{}_0D_t^{1-\gamma}c^*(x,t), \quad (17)$$

where the second line is obtained by using the Laplace transform of the Grünwald-Letnikov operator, Eq. (9), along with the explicit form (2) of  $\tilde{\psi}(u)$ . Finally, inserting Eq. (17) into Eq. (16) and expanding the abbreviated notation, we arrive at the general fractional reaction-diffusion equation that is the starting point of our analysis:

$$\frac{\partial}{\partial t}c(x,t) = K_\gamma \frac{\partial^\mu}{\partial x^\mu} \left\{ \exp \left[ - \int_0^t k(x,t') dt' \right] {}_0D_t^{1-\gamma} \left\{ \exp \left[ \int_0^t k(x,t') dt' \right] c(x,t) \right\} \right\} - k(x,t)c(x,t). \quad (18)$$

More specifically, we focus on the case  $\mu=2$  so that the spatial operator is the Laplacian, as mentioned earlier, and we also do not consider the time dependence in the degradation process. Our central starting reaction-subdiffusion equation therefore is

$$\frac{\partial}{\partial t}c(x,t) = K_\gamma \frac{\partial^2}{\partial x^2} \{ e^{-k(x)t} {}_0D_t^{1-\gamma} [e^{k(x)t} c(x,t)] \} - k(x)c(x,t). \quad (19)$$

Along with this equation, we assume a constant flux  $j_0$  of morphogens at the origin as our boundary condition. If there is a stationary state  $c_s(x)$ , then the incoming flux must be balanced by the flux of particles “away” from the system due to degradation, that is,

$$j_0 = \int_{-\infty}^{\infty} k(x)c_s(x)dx. \quad (20)$$

This condition can serve as an additional check on results.

### III. MORPHOGEN PROFILES

The solution of Eq. (19) with a constant flux  $j_0$  at the origin is related to the Green’s function or propagator  $G(x,t)$  of the problem, that is, the solution when the initial condition is a Dirac delta function at the origin,  $c(x,0) = \delta(x)$ ,

$$c(x,t) = j_0 \int_0^t G(x,t-t') dt' \quad (21)$$

or, in Laplace space,

$$\tilde{c}(x,u) = j_0 \tilde{G}(x,u)/u. \quad (22)$$

It turns out to be convenient for later manipulations to introduce a function  $v(x,t)$  defined via the transformation

$$\tilde{v}(x,u) = [u + k(x)]^{1-\gamma} \tilde{G}(x,u), \quad (23)$$

in terms of which

$$\tilde{c}(x,u) = j_0 \frac{[u + k(x)]^{1-\gamma}}{u} \tilde{v}(x,u). \quad (24)$$

The auxiliary function  $\tilde{v}(x,u)$  satisfies the ordinary differential equation

$$[u + k(x)]^\gamma \tilde{v}(x,u) - \delta(x) = K_\gamma \frac{\partial^2}{\partial x^2} \tilde{v}(x,u). \quad (25)$$

Our investigation of a number of representative reactivity profiles begins with Eq. (25).

The spatial dependence of  $k(x)$  may arise from several morphogen degradation pathways which for practical pur-

poses can be regarded as “death” or “evanescence” processes. Since the rate of each of these may depend on the local environment, we will explore the consequences of non-uniform degradation rates associated with spatially nonuniform environments [27]. As we will see below, morphogen concentration profiles turn out to depend strongly on the spatial dependence of the degradation rate. Thus, as noted earlier, the resulting morphogen gradients might provide not only a possible sensitive measure of the transport properties of the environment but also of the underlying degradation process. We next consider three degradation pathway models. The first one (constant degradation rate) has been extensively considered in the literature but only in conjunction with normal diffusive motion. The other two, piecewise constant and exponential reactivities, are chosen as simple representative models to explore the possible effects of possible more complex scenarios that are conjectured to occur but have not yet been characterized in detail [3,26].

#### A. Constant reactivity

The most commonly encountered reactivity in morphogen studies is a constant,  $k(x,t) = k$ . The solution of Eq. (25) for  $x \neq 0$  is of the form  $\tilde{v}(x,u) = A e^{-\alpha|x|} + B e^{\alpha|x|}$  with  $\alpha = (u + k)^{\gamma/2} / K_\gamma^{1/2}$ . We must choose  $B = 0$  since the solution for finite time ( $u \neq 0$ ) must be finite for  $|x| \rightarrow \infty$ . It also follows immediately that the spatial derivative of the solution is not continuous at  $x = 0$ . In fact, integrating Eq. (25) over the discontinuity at the origin leads to

$$\frac{\partial \tilde{v}(x,u)}{\partial x} \Big|_{x=0+} - \frac{\partial \tilde{v}(x,u)}{\partial x} \Big|_{x=0-} = - \frac{1}{K_\gamma} \quad (26)$$

or, equivalently, due to the even symmetry of the solution,

$$\frac{\partial \tilde{v}(x,u)}{\partial x} \Big|_{x=0+} = - \frac{1}{2K_\gamma}. \quad (27)$$

This implies that  $A^{-1} = 2(u + k)^{\gamma/2} \sqrt{K_\gamma}$  from which, using Eq. (23), it follows that

$$\tilde{G}(x,u) = \frac{1}{2} \frac{(u + k)^{\gamma/2-1}}{\sqrt{K_\gamma}} \exp[-|x|(u + k)^{\gamma/2} / \sqrt{K_\gamma}]. \quad (28)$$

From Eq. (22), one then finds the solution

$$\tilde{c}(x,u) = \frac{j_0}{2} \frac{(u + k)^{\gamma/2-1}}{u \sqrt{K_\gamma}} \exp[-(u + k)^{\gamma/2} / \sqrt{K_\gamma} |x|]. \quad (29)$$

The stationary solution is obtained from the final value theorem for the Laplace transform,

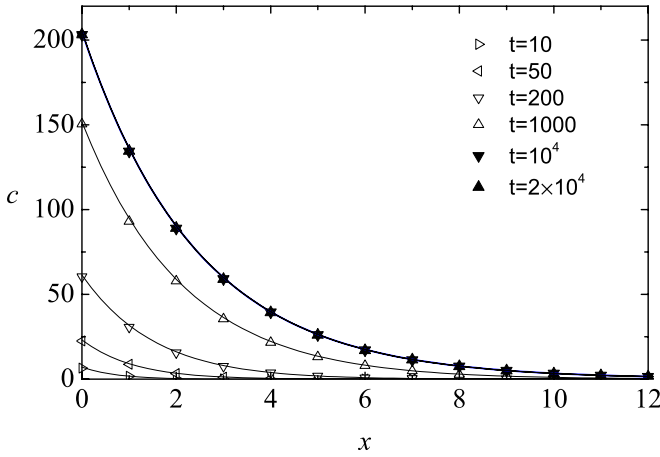


FIG. 1. (Color online) Simulation results over 1000 realizations (symbols) for  $c(x, t)$  with  $k=1/1000$ ,  $\gamma=1/2$ , and  $j_0=1$ . The particles are simulated by means of the CTRW model where the waiting time distribution is a Pareto law,  $\psi(t)=(\gamma/t_0)/(1+t/t_0)^{1+\gamma}$  with  $t_0=1$ , and the jumps  $\{-1, 0, 1\}$  are equiprobable. These parameters lead to the  $K_\gamma$ -value  $1/\sqrt{9\pi}$ . The thin lines are the profiles obtained from the inverse numerical transformation of Eq. (29). The thick line is the theoretical prediction for the steady-state profile [Eq. (30)]. There are no adjustable parameters.

$$c_s(x) = \lim_{u \rightarrow 0} u \tilde{c}(x, u) = \frac{j_0 k^{\gamma/2-1}}{2 \sqrt{K_\gamma}} \exp[-|x|/\lambda], \quad (30)$$

where the decay length is  $\lambda = \sqrt{K_\gamma/k^\gamma}$ . Equation (30) generalizes the well-known stationary exponential profile found for normal diffusion [3], which is simply this result with  $\gamma=1$ .

Because the separate determination of diffusivities and reactivities of morphogens poses significant experimental difficulties, in most cases only the exponential decay and its characteristic length  $\lambda$  can be unambiguously determined. This means that the detailed origin and parameter dependence of the gradient are experimentally uncertain [28] and opens the door to the possibility of any number of non-Markovian generalizations such as Eq. (30) that may be compatible with experimental results.

A typical time progression of the profile obtained from numerical simulations of the corresponding CTRW model is shown in Fig. 1, as are the theoretical predictions. The agreement is excellent. A steady-state profile is thus seen to exist when there is anomalous diffusion, a profile that is formally equal to that of normal diffusion.

While it may be difficult to distinguish a diffusive from a subdiffusive environment if the morphogen degradation rate is a constant independent of location, the characteristic length of the gradient does depend differently on the morphogen lifetime in the two cases ( $\lambda \sim k^{\gamma/2}$ ). If it were possible to alter the lifetime of the morphogens it would thus in principle be possible to obtain information about the nature of the environment by measuring the consequent change in the length of the gradient.

An important observation at this point is the very existence of the steady-state gradient in the case of a subdiffusive environment together with a constant rate of degradation. A

result that has been used to argue against the existence of a stationary gradient in this case [29] was obtained in [7]. However, this mainly serves to point to the importance of the detailed assumptions of the model. In our case, degradation occurs at any time, independently of whether the walker is standing still or taking a step because the two processes, degradation and spatial transitions, are assumed to be independent processes. In the work of [7] degradation occurs only in association with steps and not during waiting times, and this is insufficient to sustain a steady state.

## B. Piecewise constant reactivity

Next we consider a sequence of piecewise constant reactivities, that is, the reactivity is  $k_0$  up to some distance  $R$  from the morphogen source and it is  $k_1$  in the region  $|x| > R$ . This profile provides a simple way to model a change in the degradation mechanism across an interface or beyond a certain distance from the source. It is the simplest model that might lead to a kind of complex morphogen patterning (see below), thus providing a richer context for gene activation.

The profile can be expressed in terms of the Heaviside theta function  $\theta(x)$  which is equal to unity when  $x > 0$  and equal to zero when  $x < 0$ ,

$$k(x) = k_0 \theta(R - |x|) + k_1 \theta(|x| - R). \quad (31)$$

The most dramatic behavior for this sort of reactivity profile occurs when the reactivity is finite up to some distance and zero beyond, that is, when degradation does not occur at all for  $x > R$  ( $k_1=0$ ). In this case, the solution of Eq. (25) for  $|x| < R$  is again  $\tilde{v}(x, u) = A_0 e^{-\alpha_0 |x|} + B_0 e^{\alpha_0 |x|}$  with  $\alpha_0 = (u + k_0)^{\gamma/2} / K_\gamma^{1/2}$ . For  $|x| > R$  it is  $\tilde{v}(x, u) = A_1 e^{-\alpha_1 |x|} + B_1 e^{\alpha_1 |x|}$  with  $\alpha_1 = u^{\gamma/2} / K_\gamma^{1/2}$ . We must choose  $B_1 = 0$  since again the solution for finite time ( $u \neq 0$ ) must be finite for  $|x| \rightarrow \infty$ . Imposing the condition of continuity of the solution and its derivative at  $|x|=R$  together with the discontinuity condition [Eq. (27)] at  $x=0$  leads to

$$\begin{aligned} A_0 &= \frac{1}{2K_\gamma \alpha_0} \frac{\beta}{1 + \beta}, \\ B_0 &= -\frac{1}{2K_\gamma \alpha_0} \frac{1}{1 + \beta}, \\ A_1 &= \frac{e^{(\alpha_0 + \alpha_1)R}}{K_\gamma (\alpha_1 - \alpha_0)} \frac{1}{1 + \beta}, \end{aligned} \quad (32)$$

with  $\beta = e^{2\alpha_0 R} (\alpha_1 + \alpha_0) / (\alpha_1 - \alpha_0)$ . By means of these expressions the full solution  $\tilde{c}(x, u)$  can be evaluated using Eq. (24). The corresponding long-time solution can be straightforwardly obtained via Tauberian theorems. For  $|x| < R$  we find the stationary solution

$$c_s(x) = \frac{j_0}{2k_0} \sqrt{\frac{k_0^\gamma}{K_\gamma}} \operatorname{csch}\left(R \sqrt{\frac{k_0^\gamma}{K_\gamma}}\right) \cosh\left((x-R) \sqrt{\frac{k_0^\gamma}{K_\gamma}}\right). \quad (33)$$

As  $|x| \rightarrow R$  from below this yields a constant concentration which is then in effect a boundary condition for the solution beyond. For  $|x| > R$  the long-time solution is

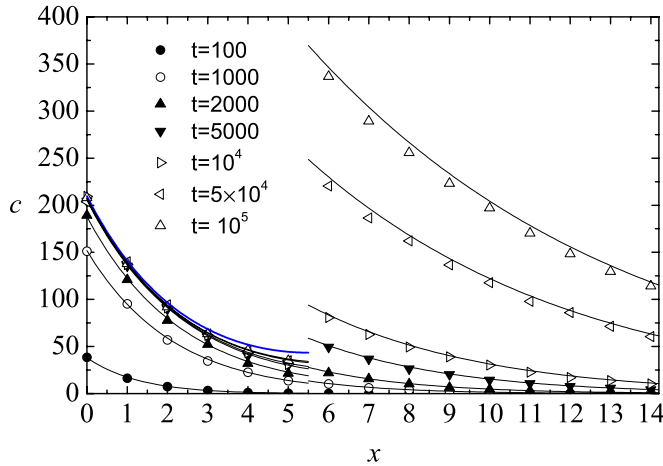


FIG. 2. (Color online) Simulation results for 50 realizations of  $c(x,t)$  (symbols) for a step reactivity  $[k(x)=k_0H(R-x)]$  with  $k_0=1/1000$ ,  $R=5.5$ , and  $j_0=1$  for  $\gamma=1/2$ . The particles are simulated as in Fig. 1. The thin lines are the profiles obtained from the inverse numerical transformation of Eq. (29). The thick solid line corresponds to the theoretical prediction for the steady-state profile when  $x < R$ . For  $x > R$  there is no stationary profile. The convergence of the simulation results to the stationary profile for  $x < R$  is very slow for values of  $x$  close to the discontinuity at  $x=R$ . No adjustable parameters were used.

$$c(x, t \rightarrow \infty) \sim \frac{j_0}{2k_0\Gamma(2-\gamma)} \sqrt{\frac{k_0^\gamma}{K_\gamma}} \operatorname{csch}\left(R \sqrt{\frac{k_0^\gamma}{K_\gamma}}\right) t^{1-\gamma}. \quad (34)$$

For normal diffusion this approaches a nonzero constant, as might be expected for a region without a reaction but with a constant concentration boundary at one end. However, for anomalous diffusion the concentration in this region grows as  $t^{1-\gamma}$ , indicating that the constant concentration boundary “feeds” morphogens into this region more rapidly than subdiffusion can carry them away and disperse them. The concentration at  $|x|=R$  thus becomes discontinuous and there is no steady state. Both of these features are confirmed by numerical simulations (see Fig. 2).

Before discussing this outcome further, we note that Fig. 2 also exhibits transient results that illustrate the approach to the long-time behavior. These results must be viewed with some caution and not with quantitative severity. The simulations are carried out on a discrete lattice and so a continuum rendition such as shown in the figure is somewhat uncertain. More specifically, the simulation results would be the same for a location of the step anywhere in the range  $5 < R < 6$ . On the other hand, the theoretical results vary as we change the location of the step, especially when the change in the concentration as a function of position is very steep. We have chosen the intermediate location  $R=5.5$  when reporting the curves in the figure. At time  $t=10^5$  and location  $x=6$ , for instance, the value of  $c$  shown in the figure is 346.4. Had we chosen  $R=5$  it would have been 399.7, with  $R=6$  it would be 300.4. Nevertheless, the trend is certainly clear.

The bottom line is this: a morphogen degradation profile such as shown for long times in the figure leads to entirely

different behaviors when the morphogen motion is diffusive or subdiffusive. Furthermore, the nonmonotonicity of the profile may have interesting biological consequences: the combined action of anomalous transport and a rapid spatial variation of the reactivity (taken to an extreme in this model) may induce nonstationary complex tissue patterning where genes in spatially distant cells are similarly expressed.

### C. Exponential reactivity profile

Here we consider  $k(x)=ke^{-\beta|x|}$  as a continuous model of rapidly decreasing reactivity as opposed to the sudden step function drop of the previous case. The morphogen reactivity might, for example, be affected by the concentration of some other substance which is itself produced by the morphogens whose concentration is decreasing with distance  $|x|$  from the source. The mathematics for dealing with a rapidly increasing reactivity ( $\beta < 0$ ) is entirely parallel but the results are not particularly revealing and so we restrict our attention to the more interesting situation of a reactivity that decreases with distance from the source.

Equation (25) does not seem exactly solvable for finite  $u$  with this reactivity profile. It is possible to arrive at an approximate solution by, for example, approximating  $[u+k(x)]^\gamma$  by  $u^\gamma+k(x)^\gamma$ , but the outcome is not especially illuminating. Instead, we focus on the steady-state profile obtained by replacing  $[u+k(x)]^\gamma$  by  $k(x)^\gamma$  in Eq. (25). This replacement is exact in the long-time limit  $u \rightarrow 0$ . The general solution  $\tilde{w}(x,u)$  of the resulting equation is a linear combination of the modified Bessel functions  $I_{\alpha u^{\gamma/2}}[\alpha k^{\gamma/2}(x)]$  and  $K_{\alpha u^{\gamma/2}}[\alpha k^{\gamma/2}(x)]$  with  $\alpha=2/(\beta\gamma\sqrt{K_\gamma})$ , but the coefficient of  $K_{\alpha u^{\gamma/2}}$  must be set to zero for the solution to remain finite as  $|x| \rightarrow \infty$  at finite times. Furthermore, the solution must also obey the discontinuity condition  $\partial\tilde{w}(x,u)/\partial x|_{x=0+} - \partial\tilde{w}(x,u)/\partial x|_{x=0-} = -1/K_\gamma$  at  $x=0$  [see Eq. (27)]. The explicit solution valid for small  $u$  (long times) then is

$$\tilde{w}(x,u) = \frac{1}{\sqrt{k_0^\gamma K_\gamma} I_{\alpha u^{\gamma/2+1}}(\alpha k_0^{\gamma/2}) + I_{\alpha u^{\gamma/2-1}}(\alpha k_0^{\gamma/2})} I_{\alpha u^{\gamma/2}}(\alpha k_0^{\gamma/2} e^{-\gamma\beta|x|/2}). \quad (35)$$

Since  $\tilde{w}(x,u)$  and  $\tilde{v}(x,u)$  coincide when  $u \rightarrow 0$ , we directly implement Eq. (24) and invert to obtain the long-time solution  $c_s(x)=c(x, t \rightarrow \infty)$ ,

$$c_s(x) = j_0 \frac{k^{\gamma/2-1} I_0(\alpha k^{\gamma/2} e^{-\beta\gamma|x|/2})}{2K_\gamma^{1/2} I_1(\alpha k^{\gamma/2})} e^{-(\gamma-1)\beta|x|}. \quad (36)$$

For normal diffusion Eq. (36) is a monotonically decreasing profile from the concentration value at the origin to a constant nonzero limiting value, which is a behavior similar to that obtained with a step function reactivity. Thus, while the reactivity here in the outlying regions is not zero, it decreases sufficiently rapidly to support a finite morphogen concentration throughout. This is shown in Fig. 3. The behavior is, however, quite different in the subdiffusive case  $\gamma < 1$ . Now as one moves away from the source, first the concentration decreases until it reaches a minimum, but then it increases as  $\exp[(1-\gamma)\beta|x|]$  (see Fig. 4). This should be compared with the behavior associated with a sudden drop of the reactivity, see Fig. 2. There the concentration diverged

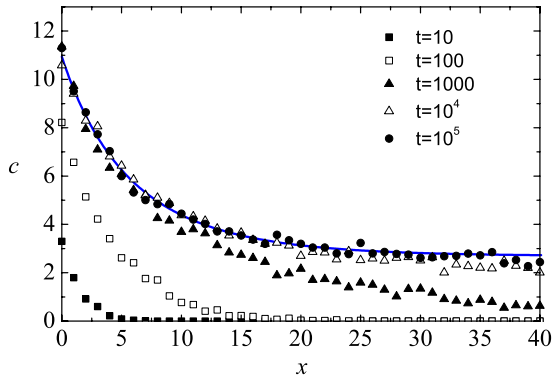


FIG. 3. (Color online) Convergence of CTRW simulation results for 50 realizations (symbols) to the stationary profile predicted by formula (36) for  $j_0=1$ ,  $\gamma=1$  (normal diffusion),  $K_\gamma=1/3$ , and exponentially decaying reactivity  $k(x)=k \exp(-\beta|x|)$  with  $k=1/100$  and  $\beta=1/8$  (solid line). The particles are simulated as in Fig. 1, but with the waiting time distribution  $\psi(t)=t_0^{-1} \exp(-t/t_0)$  with  $t_0=1$ . The simulation results clearly approach the stationary solution as time increases.

and there was no steady state. Here it increases beyond the minimum but for any value of  $x$  there is a steady-state value, albeit large for large  $x$ . While we do not have a divergence here, the nonmonotonicity of the steady-state profile arising from the combined action of anomalous transport and a sufficiently rapid spatial decrease of the reactivity may again induce interesting complex tissue patterning effects.

#### IV. ROBUSTNESS

A key property of morphogen gradients is their robustness against environmental and genetic fluctuations [30]. One way to assess the robustness of a given concentration value

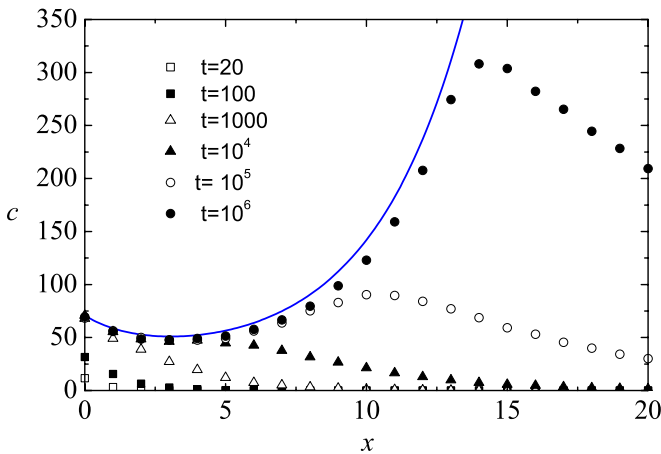


FIG. 4. (Color online) Convergence of CTRW simulation results for 50 realizations (symbols) to the stationary profile predicted by formula (36) for  $j_0=1$ ,  $\gamma=0.5$ , the corresponding value  $K_\gamma=1/\sqrt{9\pi}$  (subdiffusion) and exponentially decaying reactivity  $k(x)=k \exp(-\beta|x|)$  with  $k=1/200$  and  $\beta=0.6$  (solid line). The particles are simulated as in Fig. 1. The simulation results clearly go towards the stationary solution as time increases, although the convergence for large  $x$  is slow.

$c_s(x)$  against fluctuations in any of the parameters  $b$  of the model, e.g., the anomalous diffusion coefficient or the flux of any parameter associated with the degradation process, is to focus on the value  $x=L$  at which the concentration has the given value and find  $L$  from the relation  $L=c_s^{-1}(x)|_{x=L}$ . A standard dimensionless robustness parameter  $\mathcal{R}_b$  used to quantify the shift of the position  $L$  of the profile at a given level of concentration when  $b$  changes then is

$$\mathcal{R}_b = a \left( b \frac{\partial L}{\partial b} \right)^{-1}, \quad (37)$$

where  $a \ll L$  is a suitable characteristic length of the system (for example, the typical size of the cells) [8]. If it is desirable to have a system impervious to changes in the parameter  $b$ , then this quantity ought to be as large as possible. On the other hand, the way that this quantity varies as parameters are varied tells us whether it can be used to distinguish between different models or behaviors.

To illustrate the point, consider the robustness of the morphogen profile for a constant reactivity. In particular, consider the robustness against changes in the secreted flux,

$$\mathcal{R}_j = a \left( j_0 \frac{\partial L}{\partial j_0} \right)^{-1} = a \left( \frac{k^\gamma}{K_\gamma} \right)^{1/2}, \quad (38)$$

where we have used Eq. (30). We wish to highlight the difference in the behavior of this quantity between a diffusive and a subdiffusive environment. Because of the multiparameter dependence of the robustness, to extract the effect of  $\gamma$  we need to scale our expression in a way that isolates the  $\gamma$  dependence. We thus write  $\mathfrak{R}_j = \sigma \mathcal{R}_j / a$ . This scaled robustness is then

$$\mathfrak{R}_j = \kappa^{\gamma/2}, \quad (39)$$

where  $\kappa = k\tau$  is the degradation rate in units of  $\tau^{-1}$ . The question now is, how does this robustness (which is independent of the value of the flux itself) depend on the degradation rate? Is the subdiffusive system more or less robust against changes in the flux? We see that if the parameters  $\sigma$  and  $a$  are fixed, then the robustness itself is greater in the diffusive system when  $\kappa > 1$  and greater in the subdiffusive system when  $\kappa < 1$ . Subdiffusion thus buffers the effect of fluctuations in the flux if the degradation rate is sufficiently small compared to the reciprocal of the characteristic stepping time.

We can similarly explore the robustness against changes in the degradation rate,

$$\mathcal{R}_k = a \left( k \frac{\partial L}{\partial k} \right)^{-1} = \frac{a}{\gamma/2(1 - \ln \beta) - 1} \left( \frac{k^\gamma}{K_\gamma} \right)^{1/2}, \quad (40)$$

where  $\beta$  is the ratio of the value of the steady-state concentration at the origin and the given value of the concentration being explored (here chosen to be the concentration at  $x=L$ ), typically of the order  $e^1$ . One can again introduce a scaling that leads to a scaled robustness as in Eq. (39). The conclusions that follow are then exactly as listed above. In particular, subdiffusion again buffers the effect of fluctuations in the degradation rate if this rate is sufficiently small compared to the reciprocal characteristic stepping time.

## V. CONCLUSIONS AND OUTLOOK

We have investigated concentration profiles of morphogens that move in subdiffusive media such as the embryonic environment and are also subject to a degradation process. The degradation process may depend on location. We have assumed that the subdiffusive motion of the morphogens can be described as a CTRW and have derived a fractional reaction-subdiffusion equation starting from a CTRW model together with a death process. This formulation has allowed us to exploit a number of powerful analytical techniques available from fractional calculus. We have found that for constant reactivity a stationary exponential profile (well tested experimentally) is predicted by both normal and fractional reaction-diffusion equations, leading us to conjecture that a subdiffusive process underlying the profile might have been overlooked in some morphogenesis experiments. On the other hand, we have found morphogen profiles that exhibit effects not seen in normal diffusion. They include the absence of steady states, nonmonotonic profiles, and transitions between monotonic and nonmonotonic profiles. Analogous anomalous behavior has been obtained in entirely different contexts, specifically for stationary reaction fronts [23] and in geminate recombination reactions [18]. In the context of morphogen gradient formation, these signatures may provide essential information about the nature of the medium, about morphogen motion in the medium, and about the morphogen degradation process. We continue to explore other reactivity profiles and different boundary conditions, as well as the application of Eq. (18) to degradation processes that may depend on time and space [12,16,17]. Feedback effects in the rate of morphogen degradation (involving nonlinear degradation terms) are also extremely interesting.

It should be noted that while the conclusions reached in this paper are associated with a CTRW model of subdiffusion, other models (for example, fractional Brownian motion and diffusion in fractal media) also describe subdiffusive processes. Which model is appropriate in the context of a

particular system is a subject of intense current scrutiny [31] and includes the development of methods to distinguish diffusion from subdiffusion in experimental data [32]. The sharp and distinct results reported here may thus serve as a useful tool to discriminate not only between normal diffusive and subdiffusive morphogenesis but also between the different flavors of subdiffusive models.

We end by noting that although we have focused on morphogen gradient formation, the reaction-subdiffusion equation that we have derived and solved may be useful in other situations that involve creation of a species at a source, movement of this species through a complex medium, and simultaneous degradation. We noted that such scenarios might arise, for example, in the context of point-source pollutants in ground water. At the present stage, we view our contribution as an exploration of an approach to the problem and not as a predictive tool for specific experimental results. Some of the features that we have identified can be expected to persist even if the subdiffusive motion is described differently or if the degradation process is somewhat different from those presented here. For example, it may be a general feature of a subdiffusive environment that a degradation rate that decays sufficiently rapidly as one moves away from the source may define a situation where the morphogens or other chemical species are not carried away sufficiently rapidly, and an accumulation of some sort occurs, opening the way for a nonmonotonic concentration profile and the associated patterning possibilities. In any case, we have shown that the interplay of subdiffusion and space-dependent degradation can together lead to a wide panorama of different behaviors.

## ACKNOWLEDGMENTS

This work was partially supported by the Ministerio de Ciencia y Tecnología (Spain) through Grant No. FIS2007-60977, by the Junta de Extremadura (Spain) through Grant No. GRU09038, and by the National Science Foundation under Grant No. PHY-0855471.

- 
- [1] F. Crick, *Nature (London)* **225**, 420 (1970).
  - [2] J. B. Gurdon and P.-Y. Bourillot, *Nature (London)* **413**, 797 (2001).
  - [3] O. Wartlick, A. Kicheva, and M. González-Gaitán, *Cold Spring Harb. Perspect. Biol.* **1**, a001255 (2009); A. Kicheva, P. Pantazis, T. Bollenbach, Y. Kalaidzidis, T. Bittig, F. Jülicher, and M. González-Gaitán, *Science* **315**, 521 (2007); S. R. Yu, M. Burkhardt, M. Nowak, J. Ries, Z. Petrek, S. Scholpp, P. Schwillie, and M. Brand, *Nature (London)* **461**, 533 (2009).
  - [4] A. Eldar, D. Rosin, B.-Z. Shilo, and N. Barkai, *Dev. Cell* **5**, 635 (2003).
  - [5] M. Ibañez and J. C. Izpisua Belmonte, *Mol. Syst. Biol.* **4**, 176 (2008).
  - [6] I. Tolić-Nørrelykke, E.-L. Munteanu, G. Thon, L. Oddershede, and K. Berg-Sørensen *Phys. Rev. Lett.* **93**, 078102 (2004); I. Golding and E. C. Cox, *ibid.* **96**, 098102 (2006); J. A. Dix and A. S. Verkman, *Annu. Rev. Biophys.* **37**, 247 (2008); M. R. Horton, F. Höfling, J. O. Rädler, and T. Franosch, *Soft Matter* **6**, 2648 (2010).
  - [7] G. Hornung, B. Berkowitz, and N. Barkai, *Phys. Rev. E* **72**, 041916 (2005).
  - [8] T. Bollenbach, K. Kruse, P. Pantazis, M. González-Gaitán, and F. Jülicher, *Phys. Rev. Lett.* **94**, 018103 (2005).
  - [9] R. Metzler and J. Klafter, *Phys. Rep.* **339**, 1 (2000).
  - [10] W. M. Saltzman and W. L. Olbricht, *Nat. Rev. Drug Discovery* **1**, 177 (2002).
  - [11] R. Metzler and J. Klafter, *J. Phys. A* **37**, R161 (2004).
  - [12] A. Yadav and W. Horsthemke, *Phys. Rev. E* **74**, 066118 (2006).
  - [13] Y. Nec and A. A. Nepomnyashchy, *J. Phys. A: Math. Theor.* **40**, 14687 (2007).
  - [14] S. Eule, R. Friedrich, F. Jenko, and I. M. Sokolov, *Phys. Rev. E* **78**, 060102(R) (2008).
  - [15] S. Fedotov, *Phys. Rev. E* **81**, 011117 (2010).



- [16] V. Mendez, S. Fedotov, and W. Horsthemke, *Reaction-Transport Systems: Mesoscopic Foundation, Fronts, and Spatial Instabilities* (Springer-Verlag, Berlin, 2010), p 82.
- [17] A. Yadav, S. M. Milu, and W. Horsthemke, *Phys. Rev. E* **78**, 026116 (2008); M. O. Vlad and J. Ross, *ibid.* **66**, 061908 (2002).
- [18] K. Seki, A. I. Shushin, M. Wojcik, and M. Tachiya, *J. Phys.: Condens. Matter* **19**, 065117 (2007).
- [19] I. M. Sokolov, M. G. W. Schmidt, and F. Sagués, *Phys. Rev. E* **73**, 031102 (2006).
- [20] E. Abad, S. B. Yuste, and K. Lindenberg, *Phys. Rev. E* **81**, 031115 (2010).
- [21] S. B. Yuste and K. Lindenberg, *Phys. Rev. E* **76**, 051114 (2007); R. Borrego, S. B. Yuste, and E. Abad, *ibid.* **80**, 061121 (2009); I. M. Zaid, M. A. Lomholt, and R. Metzler, *Biophys. J.* **97**, 710 (2009).
- [22] B. I. Henry, T. A. M. Langlands, and S. L. Wearne, *Phys. Rev. E* **74**, 031116 (2006).
- [23] D. Froemberg and I. M. Sokolov, *Phys. Rev. Lett.* **100**, 108304 (2008); *Acta Phys. Pol. B* **41**, 989 (2010).
- [24] R. Gorenflo and F. Mainardi, in *Anomalous Transport*, edited by R. Klages, G. Radons, and I. M. Sokolov (Wiley-VCH, Weinheim, 2008).
- [25] I. Podlubny, *Fractional Differential Equations* (Academic Press, San Diego, 1999).
- [26] D. Ben-Zvi and N. Barkai, *Proc. Natl. Acad. Sci. U.S.A.* **107**, 6924 (2010).
- [27] T. Gregor, W. Bialek, R. R. de Ruyter van Steveninck, D. W. Tank, and E. F. Wieschaus, *Proc. Natl. Acad. Sci. U.S.A.* **102**, 18403 (2005).
- [28] O. Grimm, M. Coppey, and E. Wieschaus, *Development* **137**, 2253 (2010).
- [29] F. Tostevin, P. R. ten Wolde, and M. Howard, *PLOS Comput. Biol.* **3**, e78 (2007).
- [30] T. E. Saunders and M. Howard, *Phys. Rev. E* **80**, 041902 (2009).
- [31] Y. He, S. Burov, R. Metzler, and E. Barkai, *Phys. Rev. Lett.* **101**, 058101 (2008); M. Magdziarz, A. Weron, and K. Burnecki, *ibid.* **103**, 180602 (2009); J. Szymanski and M. Weiss, *ibid.* **103**, 038102 (2009); S. C. Weber, A. J. Spakowitz, and J. A. Theriot, *ibid.* **104**, 238102 (2010).
- [32] A. Lubelski and J. Klafter, *Biophys. J.* **94**, 4646 (2008).